Low Frequency Raman Active Vibrations in Fullerenes. 2. Quadrupolar Modes

Hans-Jürgen Eisler, Frank H. Hennrich, Stefan Gilb, and Manfred M. Kappes*

Institut für Physikalische Chemie, Universität Karlsruhe, 76128 Karlsruhe, Germany

Received: September 14, 1999

The lowest frequency Raman active (molecular) vibrations of known fullerenes are quadrupolar in nature (QP modes). They can be simply rationalized in terms of the 5-fold degenerate D_g oscillation of an isotropic spherical shell. Symmetry distortion away from spherical leads to lifting of the degeneracy and correspondingly up to five vibrational features may be resolved in the QP-mode regions of the Raman spectra of high fullerenes. The energy splitting is a measure of fullerene cage topology.

1. Introduction

In the first paper[1] of this two part series, we have demonstrated that fullerenes have a Raman active monopolar breathing mode, which can be used as a rough diagnostic for cage mass (=“surface” area). This vibration is one of several low frequency “acoustic” modes in C_{60} which can be described quite well in terms of continuum mechanics. Specifically, the $A_g(1)$ breathing mode of C_{60} correlates almost quantitatively with the S_g oscillation of an isotropic spherical shell having infinitely thin walls,[2,3] parametrized to the mechanical properties of bulk graphite.[4,5] We have argued that this surprisingly good correspondence is the result of a fortuitous combination of object size and characteristic vibrational properties. On the basis of dimensional arguments (distance travelled by sound during a vibrational period) one would expect such a continuum approach to quickly break down in going to vibrations *higher* in frequency. This is in fact observed.[3] Correspondingly *lower* frequency vibrations may still be well described. C_{60} has two Raman active[7] vibrations below the $A_g(1)$ mode: $H_g(1)$ and $H_g(2)$. Comparison to the continuum model (Figure 2 of ref 1) suggests that the $H_g(1)$ mode correlates with a D_g quadrupolar “squashing” (QP) oscillation, which corresponds to one of the two class II $l = 2$ solutions in Lamb theory.[2] This oscillation and its mapping onto quadrupolar like modes in higher fullerenes is the subject of the present paper.

2. Results and Discussion

2.1. QP Mode in C_{60}. In contrast to the breathing mode, Lamb theory does only a moderately good job at quantitatively predicting the QP mode frequency. Using the same input as in the calculation of the monopolar mode ($\omega_{l=0}$),[1] equivalent to assuming a Poisson ratio of 0.24, one can show that the frequency of the D_g quadrupolar oscillation ($\omega_{\mathrm{II}l=2(a)}$; class II, lower frequency $l = 2$ solution) of a 0.35 nm radius hollow sphere is given as $\omega = 218$ cm^{-1}. This may be compared to 269 cm^{-1} for the $H_g(1)$ mode in experiment. The reason for this ∼20% deviation may best be appreciated in terms of a tensor surface harmonic theory formulation of the vibrations in spherical molecular shells having *N*-atoms[3]. This formulation (CFV) contains both a C−C stretching (k_1) and a C−C−C bending force constant (k_2). In the limit of large N and $k_2 = 0$, CFV may be mapped onto Lamb theory. For finite k_2 the monopolar mode remains unchanged (relative to $k_2 = 0$) while the quadrupolar mode is raised in energy. Consequently, as CFV argue, the Lamb theory picture of an infinitely thin homogeneous shell in which “flexural” (=surface twisting) contributions to the oscillatory motion can be neglected is equivalent to assuming that changing C−C−C bond angles costs essentially no potential energy. This is true for monopolar modes in which C−C−C bond angles in fact do not change but not for quadrupolar vibrations—the atomic structure of the elastic sphere is already too “grainy”.

2.2. QP Modes in High Fullerenes? *2.2.1. Qualitative Considerations*. PM3 calculations and Raman measurements obtained as described in ref 1 were further analyzed in order to establish whether high fullerenes have QP derived modes. As before we made extensive use of PM3 visualizations of the vibrational motion.

It is intuitively obvious that, in contrast to the singly degenerate C_{60} $A_g(1)$ breathing mode, the 5-fold degenerate $H_g(1)$ vibration should undergo symmetry splitting as the cage distorts away from spherical/icosahedral. Consequently, one would expect a symmetry perturbed cage (=high fullerene) to manifest up to five separate squashing-like modes. This expectation is in fact borne out by the PM3 calculations and visualizations. All fullerenes studied have *as their lowest frequency vibrations* a set of up to five modes. These are clearly quadrupolar in nature. They occur in the Stokes-shift range 190−280 cm^{-1} depending on cage size and are always clearly separated in frequency from the next set of Raman active modes.

Figure 1 shows two examples: C_{70} and C_{80}. For C_{70}, which has D_{5h} molecular symmetry we find three QP modes of which two are doubly degenerate. For C_{80}, which has lower (D_2) cage symmetry, five separate QP-modes are observed. Table 1 contains the number of QP modes (and their respective degeneracies) derived from PM3 calculations for each of the fullerenes studied.

2.2.2. Semiempirical Calculations versus Raman Spectra. Agreement of (uncorrected) PM3 derived frequencies with experiment is very good as shown in Figures 2−4 which highlight the (FFT smoothed) QP mode regions (180−300 cm^{-1}) for C_{60}, C_{70}, C_{76}, C_{78} (C_{2v}, C_{2v}', and D_3), C_{80}, C_{82} (isomer mixture), and C_{84} (isomer mixture). In contrast to (higher frequency) breathing modes, the scaling of PM3 prediction to experiment is not required.

In the figures, the continuous vertical lines refer to PM3 predictions of QP modes. While Raman spectra were recorded at a number of different excitation wavelengths in this study,[1]

10.1021/jp9932618 CCC: $19.00
Published on Web 02/04/2000

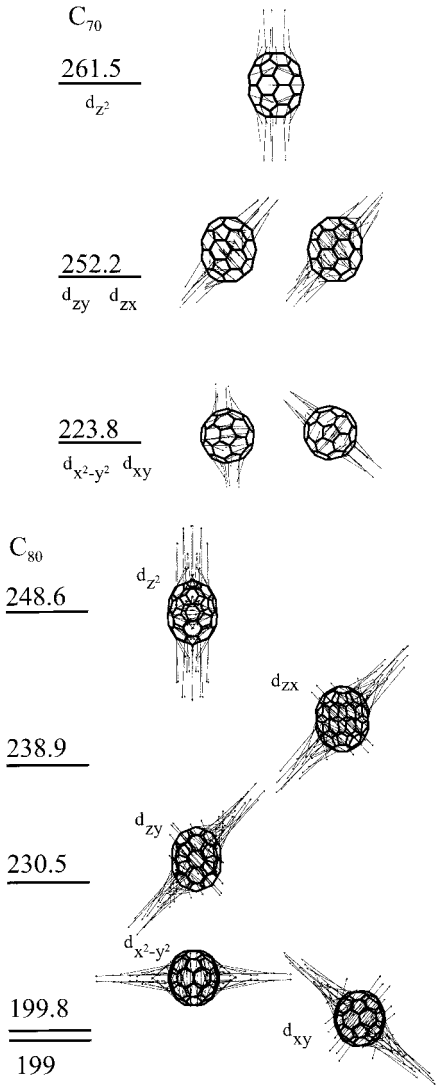

Figure 1. Visualization of symmetry split quadrupolar-like vibrations determined for C_{70} and C_{80} from PM3 calculations. Also shown are predicted frequencies in cm^{-1} and spherical harmonic parentages (expressed in terms of the respective d-orbitals), see text for details.

Figures 2−4 only show measurements at one wavelength. They can be regarded as typical insofar as the positions of resolvable QP modes were not observed to vary significantly with excitation wavelength. In contrast, relative intensities were observed to be strongly excitation wavelength dependent. Table 1 lists the corresponding experimental and PM3 frequencies. In addition to the cages studied experimentally, Table 1 also contains QP mode predictions for C_{90} and C_{140} isomers (I and D_{5d}).

In determining the experimental entries into Table 1, the number and position of Lorentzians to be deconvoluted is based on a subjective appraisal of resolved spectral features (independent of the PM3 prediction), and not on a computer-derived best fit with number of spectral features as one of the variables. Specifically, after deciding on the number and rough position of resolved features, we have varied peak maximum and Lorentzian halfwidth in order to obtain best agreement with the experimental data set. The corresponding Lorentzian fits are shown superimposed on the experimental data.

For isomer pure fullerene samples, the average (absolute) deviation between the position of deconvoluted experimental features and the corresponding PM3 predictions is less than 2 cm^{-1}. At the same time the predicted spectral range of QP features for a given fullerene agrees with the experimentally determined "width" to within an average of 2.5 cm^{-1}. Considering that no lower frequency Raman features were found either in the calculation or in the experiment (excepting noisier C_{78} measurements), assignment of experimental features to QP modes is quite straightforward (see Table 1).

TABLE 1: Quadrupole Mode Frequencies (Raman Deconvolution vs PM3 Calculations)

C_n	exptl/cm^{-1}	PM3/cm^{-1}	ν_j	nomenclature
60	271	266.5	1-5	
70	258	261.5	5	z^2
	251	252.2	3,4	*zx*, *zy*
	225	223.8	1,2	x^2-y^2, *xy*
76	250	252.7	5	z^2
	231	247.8	4	*zy*
	210	233.7	3	*zx*
		211.2	2	x^2-y^2
		208.3	1	*xy*
78 (D_3)	250	251.8	5	z^2
	238	241.5	3,4	*zy*, *zx*
	203	202.4	1,2	x^2-y^2, *xy*
78 (C_{2v})	249	245.5	5	z^2
	239	239.4	4	*zy*
	210	236.6	3	*zx*
		209.4	2	x^2-y^2
		207.5	1	*xy*
78 (C_{2v}')	242	240.7	5	z^2
	233	237.4	4	*zy*
	215	232/6	3	*zx*
		214.2	2	*xy*
		213	1	x^2-y^2
80	248	248.6	5	z^2
	238	238.9	4	*zy*
	229	230.5	3	*zx*
	202	199.8	2	*xy*
		199	1	x^2-y^2
82		no. 1, C_2		
	234	241.3	5	z^2
	221	232.5	4	*zy*
	204	229.6	3	*zx*
		200.2	2	*xy*
		199.9	1	x^2-y^2
		no. 3, C_2		
		235.4	5	z^2
		232.8	4	*zy*
		224.5	3	*zx*
		206.1	2	*xy*
		205.6	1	x^2-y^2
		D_{2d}		
84	225	222.5	5	*zx*
	220	220.3	4	*zy*
	210	219.4	3	*xy*
		219.1	2	z^2
		218.2	1	x^2-y^2
		D_2		
		227.9	5	*xy*
		227.8	4	x^2-y^2
		215.3	3	*zx*
		214.0	2	*zy*
		209.2	1	z^2
90 (D_{5h})		252.9	7	z^2
		233.9	3,4	*zy*, *zx*
		158.4	1,2	x^2-y^2, *xy*
140 (*I*)		167.6	5	*xy*
		167.5	4	x^2-y^2
		166.8	3	*zy*
		165.7	2	z^2
		165.5	1	*zx*
140 (D_{5d})		203.9	9,10	*zx*, *zy*
		198.4	8	z^2
		92.7	1,2	x^2-y^2, *xy*

2.2.3. Symmetry Splittings and Topology. We return briefly to the general expressions for class I and class II solutions of

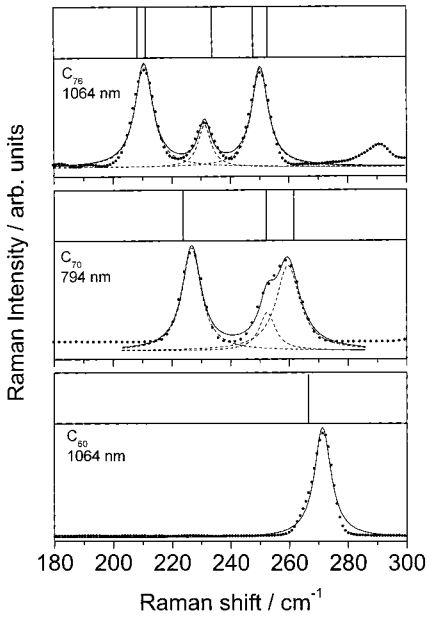

Figure 2. PM3 calculations versus Raman measurement in the low-frequency squashing mode region. Shown are spectra obtained for C_{60}, C_{70}, and C_{76}. Note the good agreement between experiment (dashed lines: Lorentzian fits) and theory (continuous vertical lines).

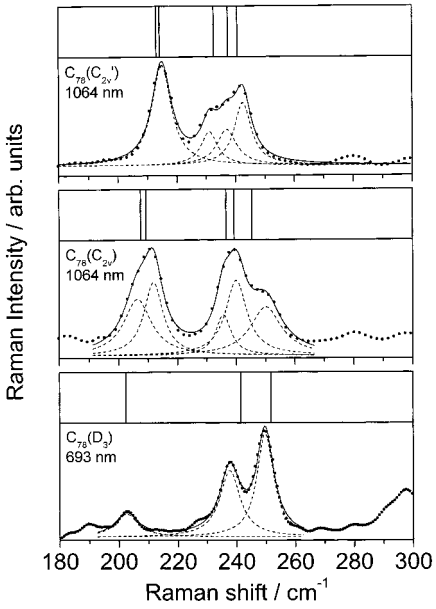

Figure 3. PM3 calculations versus Raman measurement as in Figure 2. Shown are spectra obtained for $C_{78}(C_{2v})$, $C_{78}(C_{2v'})$, and $C_{78}(D_3)$.

Lamb theory.[2] The eigenfunctions transform as the spherical harmonics. The QP mode corresponds to $l = 2$. Symmetry reduction leads to lifting of the degeneracy according to $m_l =$ 2, 1, 0, −1, and −2. In Figure 1 and Table 1 we use the analogy to d-orbitals to provide a consistent nomenclature for the various squashing modes of higher fullerenes, note that the underlying Cartesian axes correspond to the major axes of the inertial moment tensors (using the standard convention that the *z*-axis corresponds to the smallest diagonal term). Note further that while visualization of the corresponding modes derived from PM3 calculations strongly supports the analogy to d_{z^2}, $d_{x^2-y^2}$, d_{xy}, d_{zy}, and d_{zx} orbitals (see Figure 1), the vectors describing the excursions of individual atoms are not always exactly aligned with the inertial moment axes. This is a consequence of the fact that rotational ellipsoids and spheroids do not always provide a good approximation of fullerene cage topologies.

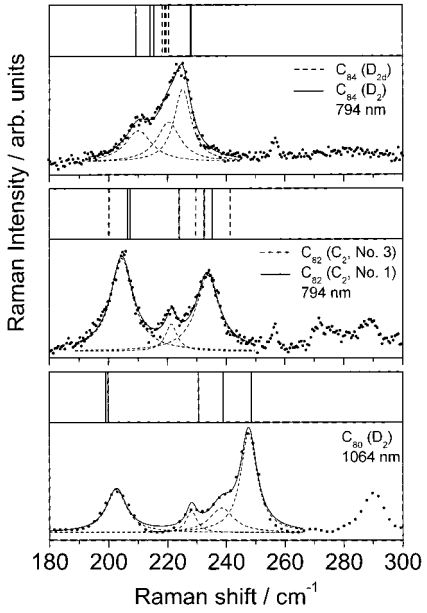

Figure 4. PM3 calculations versus Raman measurement as in Figure 2. Shown are spectra obtained for $C_{80}(D_2)$, $C_{82}(C_2+C_2)$, and C_{84}-(D_2+D_{2d}).

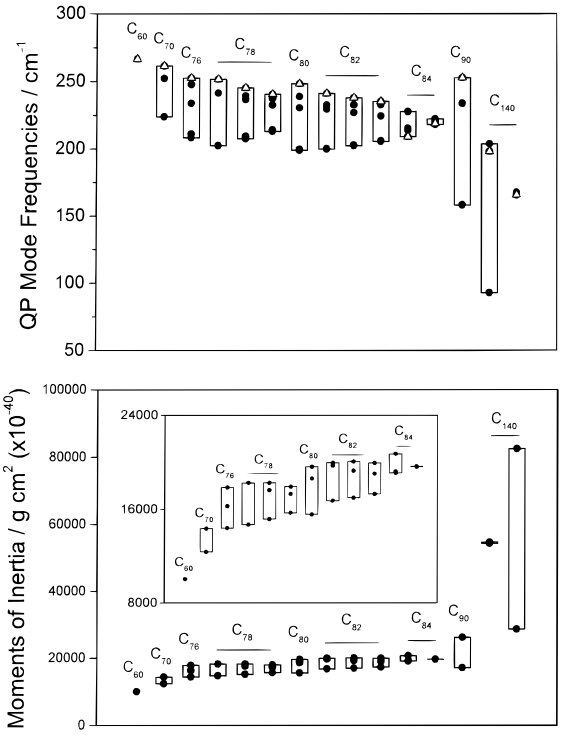

Figure 5. (a) QP mode frequencies calculated at the PM3 level for various different fullerenes. Triangles indicate "d_{z^2}" vibrations (see text); (b) Diagonal terms of the corresponding inertial moment tensors. Note the approximate correspondence between a and b.

Generally, the highest frequency QP mode corresponds to d_{z^2}. This is apparent from Figure 5, which explicitly shows all PM3 derived d_{z^2} vibrational frequencies (open triangles), in addition to all other QP frequencies for each of the fullerenes studied here. Interestingly, there is a rough correlation between deviation from spherical symmetry as quantified in terms of the diagonal terms of the respective inertial moment tensors (see Table 1 of ref 1) and the spectral range over which QP modes are observed. Highly symmetric cages always have narrow QP mode ranges ($C_{60}(I_h)$, $C_{84}(D_{2d})$ and $C_{140}(I)$) and correspondingly small numerical spreads in the diagonal terms

of the inertial moment tensor. The opposite is true for cage topologies which are highly nonspherical (e.g., tubular C_{140}-(D_{5h})). Note, however, that this correlation does not work for isomers, which differ only slightly in frequency and inertial moment spread (e.g., C_{78} or C_{82}).

Can the extent of QP mode symmetry splitting as identified in the previous section be used to roughly quantify cage topology for previously uncharacterized high fullerenes? One possible approach is to derive a global analytic formula commencing with either Lamb theory[2] or alternatively the tensor surface harmonic formalism CFV.[3] As already argued in ref 1, this might take the form of a first-order perturbation theoretical treatment (hollow sphere subject to spheroidal distortion). This is not available for either approach. We hope that our results may stimulate such work in future.

Of course while it is conceivable that such a treatment might allow for quite detailed structural characterization of cage molecules by way of a comprehensive measurement of QP modes, one still must be able to assign the latter in a situation in which relative Raman cross sections are unknown and may in fact vary strongly over the QP range. For nonresonant conditions, powder samples and unpolarized measurements one would expect QP-mode relative intensities to scale with degeneracy. A rough inspection of the 1064 nm spectra (still resonant Raman in most cases), obtained for the isomer pure samples, suggests that relative cross sections can be more than a factor of 2 outside of this expectation. However, identification is always possible because at least for the fullerene size and shape range studied here, QP modes *are always lowest frequency*, in contrast to the monopolar modes which typically fall in dense spectral regions and are therefore harder to assign unequivocally.

2.3. Isomer and Isomer Composition Assignment from Experiment/PM3 Comparison? Figure 3 documents quite pronounced "fingerprint" differences between the QP regions of the three different C_{78} isomers studied. For isomer pure samples, a Raman measurement in this spectral range would allow isomer determination. Incidentally, the 1064 nm measurement obtained for C_{80} (D_2) is in satisfactory agreement with PM3 expectation, providing further confirmation for the structural assignment.[8]

Among the high fullerene samples studied here, two (C_{82} and C_{84}) were not isomer pure. For these it is useful to consider to what degree isomer differentiation (and even composition determination) might be possible on the basis of a comparison between Raman measurement and PM3 prediction. In the case of C_{84}, independent ^{13}C NMR probes have established that the sample studied contains D_2 and D_{2d} isomers in the ratio of 2:1.[9] The resonant Raman spectrum obtained at 794 nm can best be fit in terms of three Lorentzians. Their positions and relative intensities are nominally in better agreement with the D_2 prediction with little or no contribution from D_{2d} required. However, the "spread" of predicted frequencies is quite small for both cages. One must bear in mind that compared to experiment uncorrected PM3 positions are subject to an average error of ± 2 cm^{-1} and that we have no information on the relative Raman cross sections for squashing modes in D_2 and D_{2d} isomers. Consequently, isomer differentiation by experiment/PM3 theory comparison would not have been possible in this demanding case.

For C_{82}, in contrast to C_{84}, we have no independent isomer composition determination for the sample studied. On the basis of literature reports for samples prepared analogously we assume it to be composed of two C_2 isomers (no. 1 and no. 3).[10] The measurement at 794 nm is in somewhat better agreement with the PM3 prediction for C_2 no. 3 than with C_2 no. 1. Again, resonant Raman cross sections for all possible isomers would be needed here in order to unequivocally assign the isomeric composition.

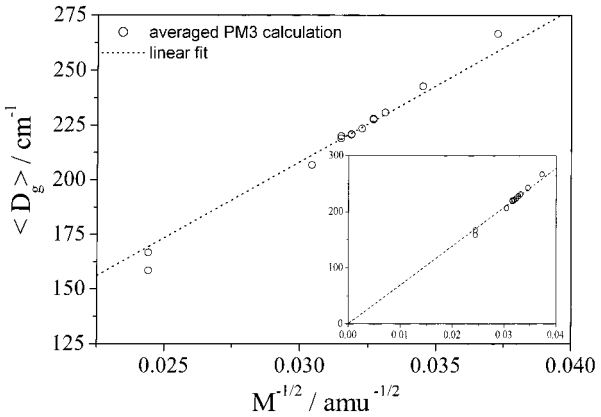

Figure 6. Average QP mode frequencies versus $M^{-1/2}$. The dotted line is a fit to the full data set constrained to go through the coordinate origin (insert shows extrapolation to $M^{-1/2} = 0$).

2.4. Global Size Trends. In both Lamb theory and CFV as applied to spherical shells, the frequency of the D_g squashing mode goes as $1/R$ where R is the shell radius.[2,3] Correspondingly PM3 quadrupolar mode frequencies calculated for C_{60} (5-fold degenerate), D_{2d}-C_{84} (average of five near-degenerate frequencies for this near-spherical isomer) and $I-C_{140}$ (average of five almost exactly degenerate frequencies) plotted versus $M^{-1/2}$ all lie roughly on a straight line. Constrained to go through the origin one obtains a good linear least-squares fit with a regression coefficient of $R^2 = 0.9996$ (see Figure 6).

For nonspherical fullerenes in the size and topology range covered, the average or weighted average (if specific frequencies are degenerate as in C_{70}) of the squashing mode frequencies cannot be fit as well by a line constrained to go through the coordinate origin. Of course, in the limit of near-infinite length tubes (SWNTs), constraining the fit line to go through the origin does not make sense. While the d_{z^2} vibration of such tubes should tend toward zero with increasing length, SWNT's are also known to have a (degenerate) *length independent* squashing mode.[11] Therefore a nonzero QP-mode average would pertain for a series of tubelets of the same diameter but increasing length.

3. Conclusions

The lowest frequency Raman allowed (molecular) vibrations of known fullerenes are quadrupolar in nature (QP modes). They can be simply rationalized in terms of the 5-fold degenerate D_g oscillation of an isotropic spherical shell. Symmetry distortion away from spherical leads to lifting of the degeneracy and correspondingly up to five vibrational features may be resolved in the QP-mode regions of the Raman spectra of high fullerenes. The extent of symmetry splitting (measured in terms of the spectral range divided by the averaged frequency) provides a first-order measure of the deviation of cage symmetry from spherical/icosahedral. Such resonant Raman spectra may be readily obtained for microgram samples, much less than required for more detailed molecular structural probes. While folded with (resonant) Raman cross sections which are unknown a priori, characterization of QP mode regions may turn out to be useful for structure/topology determination of larger fullerenes and nanotubelets. Finally, we point out that the arguments put

forward in both papers of this series apply to all closo clusters (including many inorganic substance classes of great present interest[12]).

Acknowledgment. This research was supported by the Deutsche Forschungsgemeinschaft under Sonderforschungsbereich 551 "Kohlenstoff aus der Gasphase: Elementarreaktionen, Strukturen, Werkstoffe".

References and Notes

(1) Eisler, H.-J.; Gilb, S.; Hennrich, F. H.; Kappes, M. M. *J. Phys. Chem. A* **2000**, *104*, 1762.

(2) Lamb, H. *Proc. London Math. Soc.* **1882**, *14*, 50.

(3) Ceulemans, A.; Fowler, P.; Vos, I. *J. Chem. Phys.* **1994**, *100*, 5491. Ceulemans, A.; Vos, I. *Mol. Phys*. **1991**, *72*, 1051.

(4) Dresselhaus, M.; Dresselhaus, G.; Sugihara, K.; Spain, I.; Goldberg, H.; *Graphite Fibers and Filaments*; Springer Series in Materials Science 5; Springer-Verlag: Berlin, 1988.

(5) Liu, S.; Lu, Y.-J.; Kappes, M. M.; Ibers, J.; *Science* **1991**, 254, 408. Buergi, H.; Blanc, E.; Schwarzenbach, D.; Liu, S.; Lu; Y.; Kappes, M. M. *Angew. Chem*. **1992**, *31*, 640.

(6) Clougherty, D.; J. Gorman, J. *Chem. Phys. Lett*. **1996**, *251*, 353.

(7) See also: Duval, E. *Phys. Rev. B* **1992**, *46*, 5795.

(8) Hennrich, F. H.; Michel, R. H.; Fischer, A.; Richard-Schneider, S.; S. Gilb, Kappes, M. M.; Fuchs, D.; Bürk, M.; Kobayashi, K.; S. Nagase, S. *Angew. Chem*. **1996**, *108*, 1839.

(9) Kikuchi, K.; Nakahara, N.; Wakabayashi, T.; Suzuki, S.; Shiromaru, H.; Miyake, Y.; Saito, K.; Ikemoto, I.; Kainosho, M.; Achiba, Y. *Nature* **1992**, *355*, 142. Manolopoulos, D. E.; Fowler, P. W.; Taylor, R.; Kroto, H. W.; Walton, D. R. M. *J. Chem. Soc., Faraday Trans*. **1992**, *88*, 3117.

(10) Achiba, Y.; Kikuchi, K.; Aihara, Y.; Wakabayashi, T.; Miyake, Y.; Kainosho, M. *Mater. Res. Soc. Symp. Proc*. **1995**, *359*, 3.

(11) For example, see: Saito, R.; Dresselhaus, G.; Dresselhaus, M. *Physical Properties of Carbon Nanotubes*; Imperial College Press: London, 1998; Chapter 10.

(12) For example, see: Bornhauser, P.; Calzaferri, G. *J. Phys. Chem*. **1996**, *100*, 2035. Marcolli, C.; Calzaferri, G. *J. Phys. Chem. B* **1997**, *101*, 4925. Müller, A.; Shah, S.; Bögge, H.; M. Schmidtmann, M. *Nature* **1999**, *397*, 48 as well as papers cited therein.